Crystal Structure of the Haloalkane Dehalogenase from *Sphingomonas paucimobilis* UT26[†,‡]

Jaromír Marek,*[,§,||] Jitka Vévodová,[||] Ivana Kutá Smatanová,[§,||,⊥] Yuji Nagata,[#,▽] L. Anders Svensson,[○] Janet Newman,[×] Masamichi Takagi,[#] and Jiří Damborský*[,§]

Laboratory of Biomolecular Structure and Dynamics, and Department of Inorganic Chemistry, Faculty of Science, Masaryk University, Kotlárská 2, CZ 611 37 Brno, Czech Republic, Department of Biotechnology, University of Tokyo, Yayoi, Bunkyo-ku, Tokio 113-8657, Japan, Department of Molecular Biophysics, Center for Chemistry and Chemical Engineering, Lund University, S-221 00 Lund, Sweden, and Structural GenomiX, 10505 Roselle Street, San Diego, California 92121

Received July 5, 2000; Revised Manuscript Received August 28, 2000

ABSTRACT: The haloalkane dehalogenase from *Sphingomonas paucimobilis* UT26 (LinB) is the enzyme involved in the degradation of the important environmental pollutant γ-hexachlorocyclohexane. The enzyme hydrolyzes a broad range of halogenated cyclic and aliphatic compounds. Here, we present the 1.58 Å crystal structure of LinB and the 2.0 Å structure of LinB with 1,3-propanediol, a product of debromination of 1,3-dibromopropane, in the active site of the enzyme. The enzyme belongs to the α/β hydrolase family and contains a catalytic triad (Asp108, His272, and Glu132) in the lipase-like topological arrangement previously proposed from mutagenesis experiments. The LinB structure was compared with the structures of haloalkane dehalogenase from *Xanthobacter autotrophicus* GJ10 and from *Rhodococcus* sp. and the structural features involved in the adaptation toward xenobiotic substrates were identified. The arrangement and composition of the α-helices in the cap domain results in the differences in the size and shape of the active-site cavity and the entrance tunnel. This is the major determinant of the substrate specificity of this haloalkane dehalogenase.

γ-Hexachlorocyclohexane (γ-HCH)[1] is a potent halogenated organic insecticide employed for agricultural and public health purposes since the 1940s. Because of its toxicity and long persistence in soil, most countries have prohibited the use of γ-HCH. However, there are still many contaminated sites and, because some countries are using γ-HCH for economic reasons, new sites are still continually being contaminated. *Sphingomonas* (formerly *Pseudomonas*) *paucimobilis* SS86 was isolated from an upland experimental field to which γ-HCH had been applied once a year for 12 years in succession (*1, 2*). *S. paucimobilis* UT26 is a mutant of SS86 with a resistance to antibacterial compound nalidixic acid as a genetic marker (*3*). This microorganism can use γ-HCH as the sole carbon and energy source (*4*).

Haloalkane dehalogenase LinB is the enzyme which catalyzes the conversion of 1,3,4,6-tetrachloro-1,4-cyclohexadiene to 2,5-dichloro-2,5-cyclohexadiene-1,4-diol via 2,4,5-trichloro-2,5-cyclohexane-1-ol during γ-HCH dechlorination by *Sp. paucimobilis* UT26 (*5*). In addition to cyclic dienes, LinB also converts a broad range of halogenated alkanes and alkenes to their corresponding alcohols (*6*). The dehalogenation reaction is catalyzed without oxygen or any other cofactor. The amino acid sequence of LinB showed significant similarity to two other haloalkane dehalogenases from *Xanthobacter autotrophicus* GJ10 (DhlA; refs *7* and *8*) and *Rhodococcus rhodochrous* NCIMB 13064 (DhaA, ref *9*). These three proteins belong to different specificity classes (*10*) which are evolutionary optimized for conversion of different xenobiotic compounds. The structure of DhlA has been solved by Dijkstra and co-workers (*11*−*13*), while the structure of DhaA has recently been determined by Newman (*14*). Determination of the structure of LinB, reported here, is important for the study of the adaptation of microorganisms to the biodegradation of xenobiotic compounds at the molecular level. Understanding of the structural determinants

[†] This work was supported in part by a grant-in-aid from the Ministry of Education, Science, Sports and Culture of Japan (to Y.N. and M.T.) and by grants from the Ministry of Education, Youth and Sports of the Czech Republic (to people from Brno).

[‡] The atomic coordinates have been deposited to the Brookhaven Protein Data Bank. Reference codes are 1CV2 (native LinB) and 1D07 (dibromopropane complex).

* To whom correspondence should be addressed. (J.M. at Masaryk University) E-mail: marek@chemi.muni.cz. Phone: ++420 5 411 29 411. Fax: ++420 5 412 11 214. (J.D. at Masaryk University) E-mail: jiri@chemi.muini.cz. Phone: ++420 5 411 29 377. Fax: ++420 5 412 11 214.

[§] Laboratory of Biomolecular Structure and Dynamics, Faculty of Science, Masaryk University.

[||] Department of Inorganic Chemistry, Faculty of Science, Masaryk University.

[⊥] Present address: Laboratory of Biomembranes, Faculty of Biological Sciences, University of South Bohemia, Branišovská 31, CZ 370 05 Ceské Budejovice, Czech Republic.

[#] Department of Biotechnology, University of Tokyo.

[▽] Present address: Institute of Genetic Ecology, Tohoku University, Katahira, Sendai 980-8577, Japan.

[○] Department of Molecular Biophysics, Lund University.

[×] Structural GenomiX.

[1] Abbreviations: LinB, haloalkane dehalogenase from *Sphingomonas paucimobilis* UT26; γ-HCH, γ-hexachlorocyclohexane; DhlA, haloalkane dehalohenase from *Xanthobacter autotrophicus* GJ10; DhaA, haloalkane dehalohenase from *Rhodococcus rhodochrous* NCIMB 13064; PEG, poly(ethylene glycol); w/v, weight per volume; rmsd, root-mean-square deviation; Pdol, 1,3-propanediol; DCE, 1,2-dichloroethane.

10.1021/bi001539c CCC: $19.00
Published on Web 10/27/2000

Table 1: Summary of Data and Refinement

	native	native + DBP
data set		
space group	$P2_12_12$	$P2_12_12$
a (Å)	50.26	50.23
b (Å)	71.67	71.72
c (Å)	72.70	73.32
resolution range (Å) overall	20−1.58	20−2.0
(final shell)	(1.6−1.575)	(2.13−2.0)
unique reflections	34 513	16 801
completeness (%) overall	94.2 (81.4)	86.6 (99.8)
(final shell)		
R_{merge}[a] (final shell)	0.065 (0.146)	0.113 (0.289)
final refinement statistics		
resolution range (Å)	20−1.58	20−2.0
no. of all (obsd) reflections	34 513	16 801
	(30 870)	(13 620)
R-factor[b] (%)	14.5	16.9
R_{free}[c] (relative size of set) (%)	20.4 (5)	25.8 (8)
no. of protein atoms	2301	2301
no. of water molecules	449	269
no. of substrate atoms		7
rms deviations from ideal geometry		
bond length (Å)	0.009	0.007
bond angles (deg)	2.3	1.8
improper angles (deg)	1.3	1.2
average *B*-factors (Å^2)		
main chain	9.3	20.8
side chain	13.5	23.9
water molecules	29.7	31.2
substrate		37.9

[a] $R_{merge} = \Sigma_{hkl}\Sigma_j|I_{hklj} - \langle I_{hkl}\rangle|/\Sigma_{hkl}\Sigma_j I_{hklj}$, where calculation is performed with $I/\sigma(I) > 0$. [b] *R*-factor $= \Sigma||F_o| - k|F_c||/\Sigma|F_o|$, where $|F_o|$ and $|F_c|$ are the observed and calculated structure factor amplitudes respectively and calculation is performed with observed $[|F_o| > 4\sigma(F_o)]$ reflections only. [c] R_{free} was calculated using a random set of reflections which were omitted during refinement.

of activity and specificity of haloalkane dehalogenases will further facilitate the attempts to modify these enzymes for bioremediation purposes.

MATERIALS AND METHODS

Crystallization and Data Collection. The molecular cloning, expression, and crystallization of LinB were described elsewhere (*15*). In brief, the best crystals were obtaining by using microseeding, the hanging-drop vapor-diffusion method at 278 K and a precipitant containing 18−20% (w/v) poly(ethylene glycol) M_r 6000 (PEG 6000), 0.2 M calcium acetate and 0.1 M Tris-HCl, pH 8.9.

For data collection with native protein, a single crystal of LinB was mounted in a nylon cryoloop (Hampton Research), immersed in cryoprotectant, 20% (w/v) PEG 6000, 10% (w/v) sucrose, 10% (v/v) PEG 400, for a few seconds and then rapidly exposed to a cold nitrogen stream (Oxford Cryostream Cooler) at the crystallographic beamline BL711 at the MAX-II synchrotron in Lund (Sweden). The data were collected at 100.0 K and a wavelength of $\lambda = 0.9420$ Å using a Mar345 image plate detector (X-ray Research). To locate the LinB active site, we performed another data collection, after soaking LinB single crystals for 4 h in the reservoir solution with 25 mM 1,3-dibromopropane (DBP) added, at 278 K. The rest of experimental setup was the same as the one used for the native crystal with the exception of the wavelength ($\lambda = 0.9000$ Å). The data were processed, reduced, and merged using the XDS system (*16*) and the CCP4 suite (*17*). Results are summarized in Table 1.

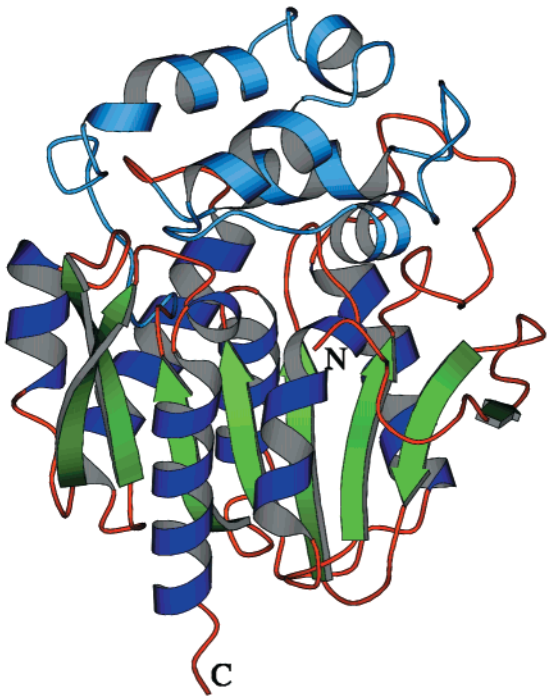

FIGURE 1: Overview of the tertiary structure of LinB. α-Helices and turns from the core domain are shown in dark-blue and red, while the helices and loops from the top domain are light-blue. All figures were generated by BobScript (*34*).

Structure Determination and Refinement. The LinB structure was solved by molecular replacement using AmoRe (*18*). During the search with the coordinates of the haloalkane dehalogenase from a *Rhodococcus* species (ref *14*; PDB entry 1BN6), we found one solution well above the background (correlation coefficient = 0.47, $R = 46\%$ for 10−4 Å data). The model was refined first by rigid body refinement using CNS (ref *19*, $R = 45\%$ and $R_{free} = 49\%$ for data between 20 and 3.0 Å data) and then by the "warpNtrace" (*20*) procedure using ARP/wARP. The resulting $2F_o - F_c$ electron density map had excellent quality and allowed us to build eight noncontinuous main-chains through 275 residues and to localize positions of 205 side chains using the program O (*21*). Refinement and model rebuilding proceed with the restrained maximum-likelihood method of the program REFMAC (*22*). Water molecules were placed into the electron density with the solvent building regime of ARP and manually checked for their correctness. In the final rounds of refinement, we used a restrained weighted conjugate-gradient method on the basis of F^2 in the program SHELXL-97 (*23*). The final model contained 2301 non-hydrogen protein atoms and 449 water molecules and converged to an *R* and R_{free} (*24*) of 14.9 and 21.1% for all experimental data (20.0−1.58 Å) and 14.5 and 20.4% for observed $[F > 4\sigma(F)]$ reflections. The main-chain dihedral angles of all residues are within the energetically allowed regions of the Ramachandran plot—88.2% of the amino acids lie in the most favored region of the plot and only two residues (Arg20 and Asp108) are in the generally allowed region.

The structure of the LinB-DBP complex was refined starting with the native LinB structure as input model using the programs REFMAC, ARP/wARP, and SHELXL-97 in the same manner as the LinB structure. The 1,3-propanediol product and two Br ion positions were localized in a σ_A-

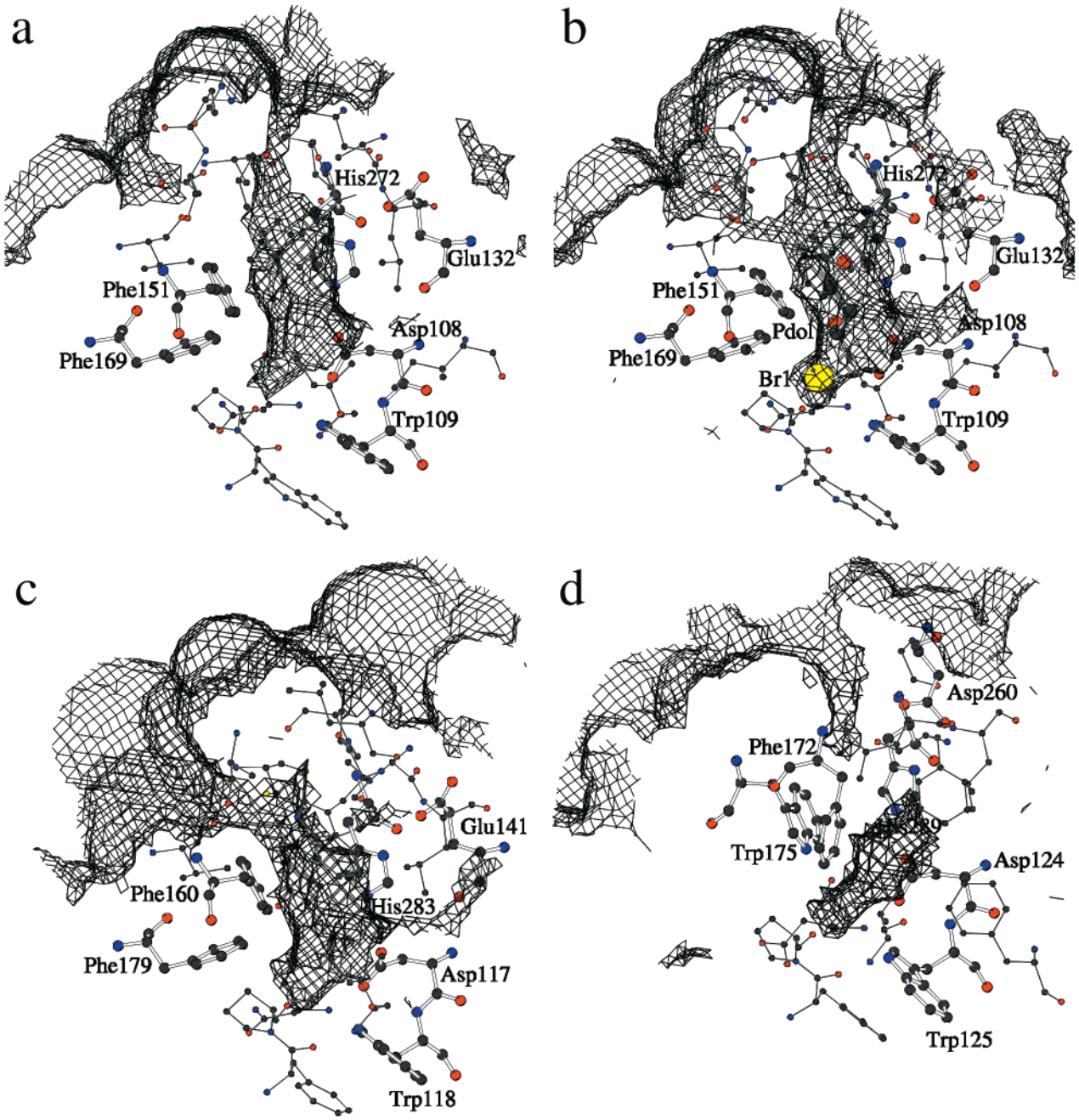

FIGURE 2: VOIDOO (*35*) and BobScript representation of the active site cavities of (a) LinB dehalogenase, (b) complex of LinB with 1,3-propanediol and 2 Br ions, products of dehalogenation of 1,3-dibrompropane, (c) *Rhodococcus* dehalogenase DhaA, and (d) *Xanthobacter* dehalogenase DhlA. The surfaces were generated with a probe radius 0.9 Å. Note the opening of the secondary entrance in enzyme−product complex of LinB (b) in position corresponding to the entrance in DhaA (c).

weighted (ref *25*) $(2m|F_{obs}| - D|F_{calc}|)\exp(i\alpha_{calc})$ electron density map at 2.0 Å resolution. During the refinement R/R_{free} decreased to 16.9/27.4% for all experimental data and to 15.9/25.8%, for the observed $[F > 4\sigma(F)]$ reflections. The final model contains 2301 non-hydrogen protein atoms, 278 water molecules and seven substrate atoms.

RESULTS AND DISCUSSION

Structure of the LinB Dehalogenase. The structure of LinB has been solved to 1.58 Å resolution, by molecular replacement using the *Rhodococcus* dehalogenase DhaA (*14*) as a search model. Crystallographic data are summarized in Table 1. The structure shows clear electron density from residue 4 to the C-terminal residue 296.

The overall structure of LinB is very similar to those of the other two structurally known dehalogenases; the root-mean-square deviation (rmsd) of 229 equivalent C_α atoms of LinB and DhlA is 1.7 Å, the rmsd of 264 C_α atoms of LinB and DhaA is 1.1 Å. The molecule is composed of two domains as shown in Figure 1. The core domain comprises residues 3−132 and 214−296 and shows the typical features of an α/β-hydrolase protein (*26*). It consists of a central twisted eight-stranded β-pleated sheet [β-strands a, b, d, c, f, g, h, and i with directions +, −, +, +, +, +, + and +, respectively], that is flanked on both sides by α-helices, two on one side and four on the other side of the sheet. Domain II, residues 133−213, consists of five α-helices and lies such as a cap on top of the core domain.

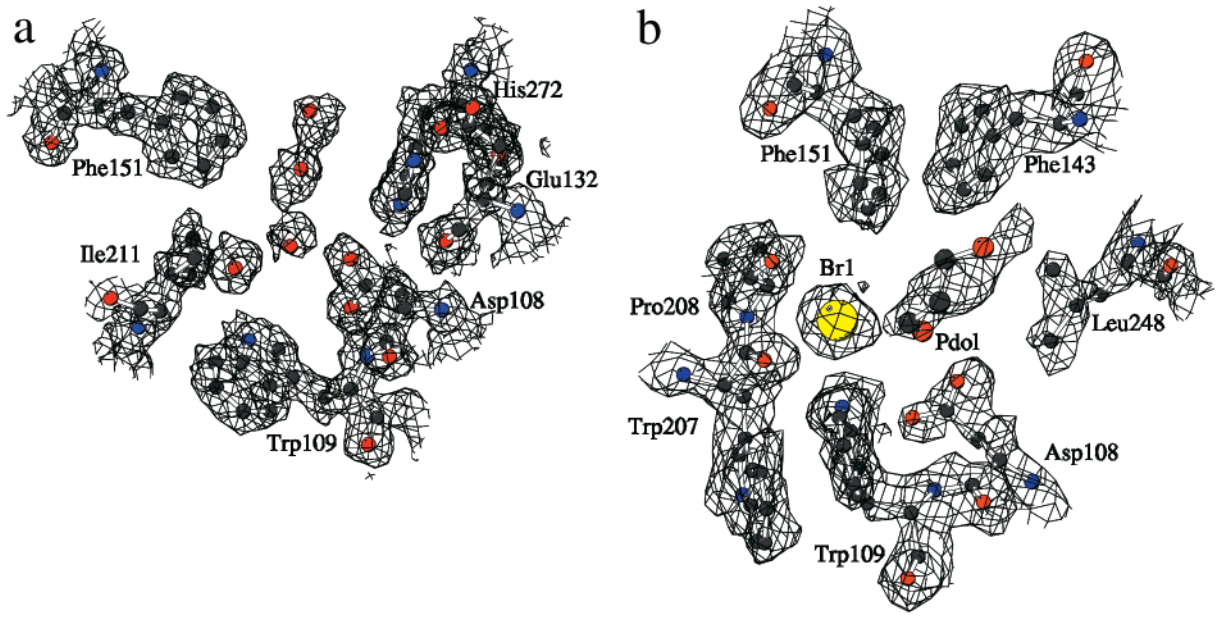

FIGURE 3: View of a part of (a) the LinB dehalogenase, and (b) complex of LinB with products of dehalogenation of 1,3-dibromopropane, $(2m|F_{obs}| - D|F_{calc}|)\exp(i\alpha_{calc})$ electron density map, contoured at 1.0σ level.

Active Site. The structure of LinB confirms the location of the catalytic triad previously proposed from site-directed mutagenesis experiments (*27*). The nucleophile Asp108 is located at the turn between β-strand β_5 and helix α_3, the base His272 is positioned in the loop joining β_8 and α_{11}, and the catalytic acid Glu132 is located after β-strand β_6. The elements of the triad are well-conserved among dehalogenases: the values of the rmsd of the 27 equiv triad atom positions in LinB and DhaA and of the rmsd of the 18 equiv atoms in LinB and DhlA are 0.4 Å. The active site of LinB is further composed of residues of helix α_4 (Gln146, Asp147, and Phe151), α_6 (Phe169, Val173, and Leu177), and α_8 (Trp207, Pro208, and Ile211), by the turn between β_5 and α_3 (nucleophile Asp108 and Trp109), the turn between β_6 and α_4 (the catalytic acid Glu132 and Ile134) and the ends of loops prior to α_4 (Phe143 and Pro144), α_{10} (Ala247 and Leu248), and α_{11} (His272 and Phe273). In contrast to the cavity in DhlA, the LinB cavity is not blocked, but is connected to the surface of the molecule by a tunnel (Figure 2). The cavity is relatively long and more or less straight (with the exception of a bend at its entrance). The distance from a water molecule, lying in the entry of the tunnel, to the end of the cavity is more than 13 Å.

Structure of the Complex of LinB with Products of Debromination. We performed a diffraction experiment not only with native LinB crystals, but also with a complex of LinB with 1,3-dibromopropane (DBP), a good substrate of LinB. LinB single crystals were soaked for 4 h in reservoir liquor with 25 mM DBP added at 278 K before data collection. Despite of the short time of exposure of the LinB crystal to DBP and the high resistance of 1-bromo-3-propanol to dehalogenation in solution (Hynková and Damborský, unpublished results), the bound substrate molecule was fully dehalogenated. We found electron density (Figure 3) corresponding to one molecule of 1,3-propanediol (Pdol) and two Br anions, the first in the active-site cavity and the second bound at the surface of the enzyme. The overall similarity between the structure of LinB and the LinB complex is very high—the rmsd between 293 C_α atoms and all 2301 atoms, respectively, is 0.2 and 0.3 Å, respectively. However, the complex active-site cavity reveals some changes. Small, but significant changes of side-chains of helix α_6 have created of a new, addition entrance to the active-site cavity. The position and the shape of this new narrow entrance tunnel in the LinB complex are very similar to the much wider tunnel to the active site cavity in the DhaA structure.

Structural Comparison of the Dehalogenases. The LinB structure was compared with the experimental structures of DhlA and DhaA in order to identify the structural determinants of their substrate specificity. The preferences of LinB and DhaA for long-chain and β-substituted haloalkanes together with their inability to dehalogenate 1,2-dichloroethane are the most obvious differences compared to the specificity of DhlA (*6*). The main domain, forming the core of all α/β-hydrolases, is sequentially and structurally conserved in all three dehalogenases in contrast to the cap domain which shows pronounced differences in the spatial arrangement of the participating secondary elements. The prominent role of the cap domain of DhlA in specificity has been proposed by Pries and co-workers, based on an analysis of in vivo mutants selected for growth on 1-chlorohexane (*28*). The cap domain participates in the lining of the active-site cavity and its anatomy directly influences the size and shape of the cavity. The active sites of LinB and DhaA are much larger and less buried than the active site of DhlA as already predicted from the homology models of LinB and DhaA dehalogenases (*29*). The volumes of the cavities calculated by CAST (*30*) are 276, 246, and 112 $Å^3$, respectively. The tunnel opening of LinB (Figure 2, panels a and b) and DhaA (Figure 2c) is formed by helices α_4, α_5, and α_6 in an U-shaped arrangement and is considerable wider than the opening of DhlA formed by helices α_5 and α_6 in a V-shaped arrangement (Figure 2d). The size of the active site and the tunnel openings correspond well with the preference of LinB and DhaA for larger substrates. The less buried active site of LinB and DhaA cannot efficiently bind 1,2-dichloroethane (DCE) resulting in inability of these enzymes to dehalogenate this substrate. Another structural

feature possibly contributing to the inactivity of LinB with DCE is the insufficient stabilization of the leaving halogen atom of the substrate during carbon−halogen bond cleavage. Experimental (*31*) and computational (*32*) mutagenesis of the halide binding residues of DhlA (Trp125 and Trp175) demonstrated the essential role of the partially positively charged nitrogen-bound hydrogens for efficient stabilization of the transition state of the first reaction step and catalytic activity of this enzyme with DCE. Trp125 of DhlA is fully conserved in LinB (Trp109) and DhaA (Trp107) structures, while the second halide-stabilizing tryptophan is present in the active site of neither LinB nor DhaA. Stabilization provided by Trp175 of DhlA is probably fulfilled by Phe169 in LinB and Phe168 in DhaA. Stabilization of the leaving halogen by Phe is however significantly less efficient than stabilization by Trp (*33*). Another halide stabilizing residue in LinB and DhaA is Asn38 and Asn41, respectively.

ACKNOWLEDGMENT

J.M. thanks the Svenska Institutet for his scholarship.

REFERENCES

1. Wada, H., Senoo, K., and Takai, Y. (1989) *Soil Sci. Plant Nutr. 35*, 71−7.
2. Senoo, K., and Wada, H. (1989) *Soil Sci. Plant Nutr. 35*, 79−87.
3. Imai, R., Nagata, Y., Fukuda, M., Takagi, M., and Yano, K. (1991) *J. Bacteriol. 173*, 6811−9.
4. Nagata, Y., Miyauchi, K., and Takagi, M. (1999) *J. Ind. Microbiol. Biotechnol. 23*, 380−90.
5. Nagata, Y., Nariya, T., Ohtomo, R., Fukuda, M., Yano, K., and Takagi, M. (1993) *J. Bacteriol. 175*, 6403−10.
6. Nagata, Y., Miyauchi, K., Damborský, J., Manová, K., Ansorgová, A., and Takagi, M. (1997) *Appl. Environ. Microbiol. 63*, 3707−10.
7. Keuning, S., Janssen, D. B., and Witholt, B. (1985) *J. Bacteriol. 163*, 635−39.
8. Janssen, D. B., Pries, F., van der Ploeg, J., Kazemier, B., Terpstra, P., and Witholt, B. (1989) *J. Bacteriol. 171*, 6791−9.
9. Kulakova, A. N., Larkin, M. J., and Kulakov, L. A. (1997) *Microbiology 143*, 109−15.
10. Damborský, J., Nyandoroh, M., Nemec, M., Holoubek, I, Bull, A., and Hardman, D. (1997) *Biotechnol. Appl. Biochem. 26*, 19−25.
11. Franken, S. M., Rozeboom, H. J., Kalk, K. H., and Dijkstra, B. W. (1991) *EMBO J. 10*, 1297−302.
12. Verschueren, K. H. G., Franken, S. M., Rozeboom, H. J., Kalk, K. H., and Dijkstra, B. W. (1993) *J. Mol. Biol. 232*, 856−72.
13. Ridder, I. S., Rozeboom, H. J., and Dijkstra, B. W. (1999) *Acta Crystallogr., Sect. D 55*, 1273−90.
14. Newman, J., Peat, T. S., Richard, R., Kan, L., Swanson, P. E., Affholter, J. A., Holmes, I. H., Schindler, J. F., Unkefer, C. J., and Terwilliger, T. C. (1999) *Biochemistry 38*, 16105−14.
15. Smatanová, I., Nagata, Y., Svensson, L. A., Takagi, M., and Marek, J. (1999) *Acta Crystallogr., Sect. D 55*, 1231−3.
16. Kabsch, W. (1993) *J. Appl. Crystallogr. 26*, 795−800.
17. Bailey, S (1994) *Acta Crystallogr., Sect. D 50*, 760−3.
18. Navaza, J. (1994) *Acta Crystallogr., Sect. A 50*, 157−63.
19. Brunger, A. T., Adams, P. D., Clore, G. M., DeLano, W. L., Gros, P., Grosse-Kunstleve, R. W., Jiang, J.-S., Kuszewski, J., Nilges, N., Pannu, N. S., Read, R. J., Rice, L. M., Simonson, T., and Warren, G. L. (1998) *Acta Crystallogr., Sect. D 54*, 905−21.
20. Perrakis, A., Morris, R., and Lamzin, V. S. (1999) *Nat. Struct. Biol. 6*, 458−63.
21. Jones, T. A., Zou, J. Y., Cowan, S. W., and Kjeldgaard, M. (1991) *Acta Crystallogr., Sect. A 47*, 110−9.
22. Murshudov, G. N., Vagin, A. A., and Dodson, E. J. (1997) *Acta Crystallogr., Sect. D 53*, 240−55.
23. Sheldrick, G. M., and Schneider, T. R. (1997) *Methods Enzymol. 277* 319−43.
24. Brünger, A. T. (1992) *Nature 355*, 472−4.
25. Read, R. J. (1986) *Acta Crystallogr., Sect. A 42*, 140−9.
26. Ollis, D. L., Cheah, E., Cygler, M., Dijkstra, B., Frolow, F., Franken, S. M., Harel, M., Remington, S. J., Silman, I., Schrag, J., Sussman, J. L., Verschueren, K. H. G., and Goldman, A. (1992) *Protein Eng. 5*, 197−211.
27. Hynková, K., Nagata, Y., Takagi, M., and Damborský, J. (1999) *FEBS Lett. 446*, 177−81.
28. Pries, F., Vanden Wijngaard, A. J., Bos, R., Pentenga, M., and Janssen, D. B. (1994) *J. Biol. Chem. 269*, 17490−4.
29. Damborský, J., and Koča, J. (1999) *Protein Eng. 12*, 989−98.
30. Liang, J., Edelsbrunner, H., and Woodward, C. (1998) *Protein Sci. 7*, 1884−97.
31. Kennes, C., Pries, F., Krooshof, G. H., Bokma, E., Kingma, J., and Janssen, D. B. (1995) *Eur. J. Biochem. 228*, 403−7.
32. Damborský, J., Kutý, M., Němec, M., and Kŏca, J. (1997) *J. Chem. Inf. Comput. Sci. 37*, 562−8.
33. Damborský, J., Boháč, M., Prokop, M., Kutý, M., and Koča, J. (1998) *Protein Eng. 11*, 901−7.
34. Esnouf, R. M. (1999) *Acta Crystallogr., Sect. D 55*, 938−40.
35. Kleywegt, G. J., and Jones, T. A. (1994) *Acta Crystallogr., Sect. D 50*, 178−85.

BI001539C